Design and fabrication of a terminating type MEMS microwave power sensor*

Xu Yinglin(许映林) and Liao Xiaoping(廖小平)†

(Key Laboratory of MEMS of Ministry of Education, Southeast University, Nanjing 210096, China)

Abstract: A terminating type MEMS microwave power sensor based on the Seebeck effect and compatible with the GaAs MMIC process is presented. An electrothermal model is introduced to simulate the heat transfer behavior and temperature distribution. The sensor measured the microwave power from –20 to 20 dBm up to 20 GHz. The sensitivity of the sensor is 0.27 mV/mW at 20 GHz, and the input return loss is less than –26 dB over the entire experiment frequency range. In order to improve the sensitivity, four different types of coplanar waveguide (CPW) were designed and the sensitivity was significantly increased by about a factor of 2.

Key words: MEMS; MMIC; microwave power; return loss; sensitivity
DOI: 10.1088/1674-4926/30/4/044010 **EEACC:** 2575; 8460

1. Introduction

Microwave power plays an important role in wireless applications and communication systems. A sensor with high sensitivity, which can measure power accurately and quickly, is needed. Thermocouple-based power sensors have been one of the most widely used tools for microwave power detection. These sensors employ the principle of the conversion of electric power to heat, which is then indirectly measured. By now, several structures of microwave power sensors have been introduced[1–3]. Most of these sensors were fabricated using a CMOS process. However, the thermal loss and lossy nature in the silicon substrate at microwave frequencies are considerable. Thus, these sensors cannot be integrated with MMICs and other planar connecting circuit structures. With the development of MEMS technology, high-precision, low-cost MEMS microwave power sensors are available. In this paper, the theory, fabrication and measurement of a terminating type microwave power sensor based on MEMS technology are presented. Its fabrication is compatible with the GaAs MMIC process. High thermal resistivity and low electromagnetic loss at microwave frequencies can be obtained using the GaAs MMIC process. Micromachining technology was used to realize the selective etching of the substrate beneath the device. By using MEMS technology and the MMIC process, the losses mentioned above are minimized. In addition, an electrothermal model is introduced to simulate the heat transfer behavior and temperature distribution, and the simulation result for the sensitivity is given.

2. Principle and model

The structure of the microwave sensor is shown in Fig. 1. A CPW feeds the microwave signal to the sensor. The CPW is designed to have a characteristic impedance of 50 Ω. It is terminated with resistive loads, which are matched to the characteristic impedance. The loads absorb the microwave power and convert it into heat. The resulting temperature increase of the loads is detected by the integrated thermocouples, which generate a DC voltage based on the Seebeck effect. The output voltage is proportional to the microwave power. The output voltage and sensitivity of the thermoelectric microwave power sensor are represented, respectively, as

$$V_{\text{out}} = \alpha \sum_{i}^{N} (T_{\text{h}} - T_{\text{c}}), \tag{1}$$

$$S_{\text{th}} = V_{\text{out}}/P_{\text{diss}}, \tag{2}$$

where α is the Seebeck coefficient, P_{diss} is the microwave power dissipated by the matched loads, N is the index of the thermocouples, T_{h} and T_{c} are the temperatures of the hot and cold junction of each thermocouple, respectively.

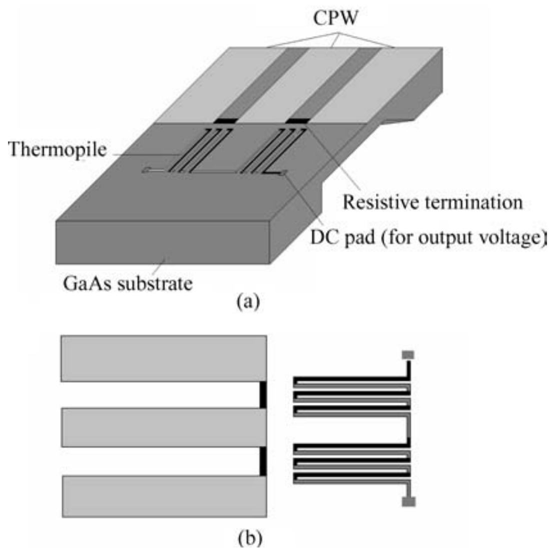

Fig. 1. (a) Schematic view and (b) top view of the microwave power sensor.

* Project supported by the National Natural Science Foundation of China (No. 60676043) and the National High Technology Research and Development Program of China (No. 2007AA04Z328).

† Corresponding author. Email: xpliao@seu.edu.cn

Received 16 September 2008, revised manuscript received 27 November 2008

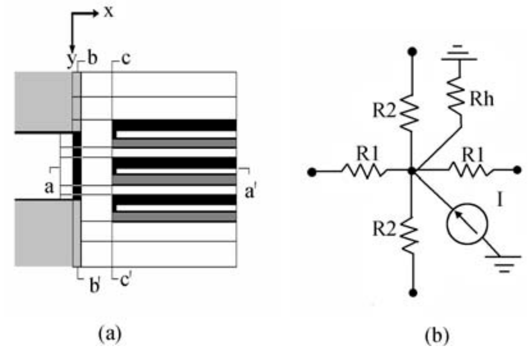

Fig. 2. (a) Schematic view of the microwave power sensor; (b) Equivalent electrical circuit including convection, conduction, and heat generation.

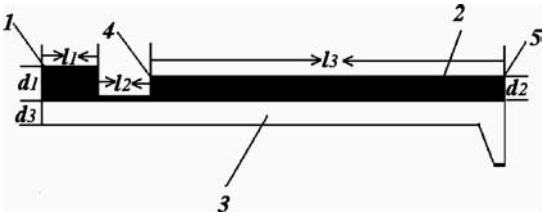

Fig. 3. Cross section view of the microwave sensor: 1. Resistive load; 2. Thermocouple; 3. GaAs substrate; 4. Hot junction; 5. Cold junction.

Figure 1(a) shows that selective etching of the GaAs substrate was used to release the high-thermally resistive membrane region underneath the resistors and the thermopile. This helped to increase the temperature gradient between the loads and the cold junctions located on the substrate, which was not etched. As a result, the sensitivity of the thermocouples was improved.

In Refs. [4, 5], the thermal conduction and convection equations were translated into circuit elements and subsequently solved using SPICE. The thermal flow was represented by a current, and the temperature by a voltage. In this work, the SPICE equivalent circuit is used to model the heat transfer behavior and the sensor temperature distribution. In addition, the thickness of the membrane is much smaller than the dimensions of the sensor. Therefore, the steady-state heat transfer is considered in the x–y coordinate system. Due to the symmetrical structure, only half of the power sensor should be considered. The 2D layout is further subdivided into smaller elements, as shown in Fig. 2(a). Each element is then represented as the equivalent circuit in Fig. 2(b). The current source is only applicable for the resistive load which dissipates power and generates heat. The conductive transfer is represented by a thermal resistor,

$$R_{1,2} = l/\lambda A, \tag{3}$$

where l is the length, λ is the thermal conductivity, and A is the cross section area. The convective resistor is

$$R_{\rm h} = 1/hA_{\rm s}, \tag{4}$$

where h is the heat-transfer coefficient, and $A_{\rm s}$ this time is the surface area. The symbol for ground in Fig. 2(b) represents the ambient temperature, i.e., 300 K in this paper.

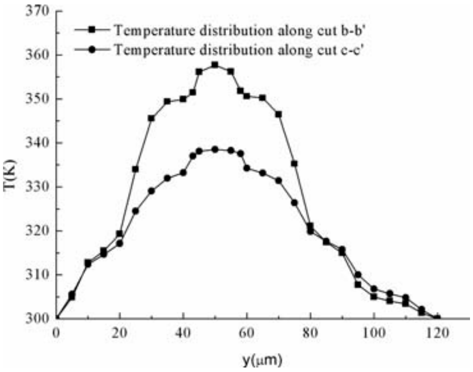

Fig. 4. Temperature distribution along the cut b–b' and cut c–c', as shown in Fig. 2(a).

The cross-sectional view of the microwave sensor is shown in Fig. 3. The symbols d_1, d_2, and d_3 are the thicknesses of the resistive load, the thermocouple, and the GaAs substrate, respectively. l_1 is the width of the resistive load. l_2 is the distance between the hot junction and the load. l_3 is the length of the thermocouple. Because the 3D structure is treated as 2D in the layout plane, the thermopile and the substrate should be regarded as one material. The same holds true for the resistive load and the substrate. In this work, some equivalent quantities used in Refs. [6, 7] are introduced. $\lambda_{\rm e1}$ is the equivalent thermal conductivity of the resistive load and the substrate, while $\lambda_{\rm e2}$ denotes the equivalent thermal conductivity of the thermopile and the substrate. They can be defined as

$$\lambda_{\rm e1} = \frac{\lambda_1 d_1 + \lambda_3 d_3}{d_1 + d_3}, \tag{5}$$

$$\lambda_{\rm e2} = \frac{\lambda_3 d_3 + \lambda_2 \frac{d_2}{2}}{d_{\rm e}} = \frac{\lambda_3 d_3 + \lambda_2 \frac{d_2}{2}}{d_3 + \frac{d_2}{2}}, \tag{6}$$

where $d_{\rm e}$ is the equivalent thickness of the thermopile and the substrate, and $\lambda_2 = (\lambda_{\rm p} + \lambda_{\rm n})/2$ is the average thermal conductivity of the thermocouple with $\lambda_{\rm p}$ and $\lambda_{\rm n}$ denoting the thermal conductivity of the positive and negative conductors of the thermocouple, respectively.

For the simulation, the constant current source was set to 100 mA, equal to an input microwave power of 20 dBm for the sensor.

After running the SPICE simulation, the equivalent circuit models the temperature distribution of the sensor. Figure 4 shows the symmetrical temperature distribution along the center cut b–b' and the hot junctions c–c'. The highest values of the temperature are in the middle and the peak value is nearly 357 K. The temperature distribution along the hot junctions is similar to that of the cut b–b', but the peak value is less than 339 K. In Fig. 5, the temperature distribution along the center cut a–a' is an approximately linear decline. From the simulation results of the temperature distribution, the sensitivity can be computed by using Eqs. (1) and (2). The sensitivity is approximately 0.32 mV/mW. By using the model, the appropriate dimensions of the layout of the sensor can be obtained depending on the required sensitivity.

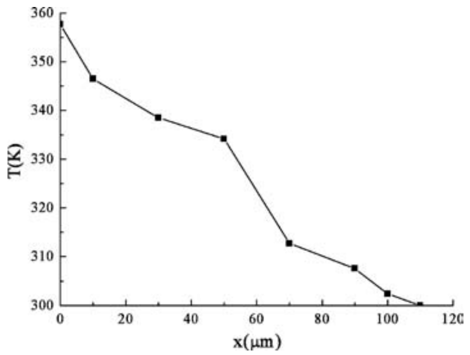

Fig. 5. Temperature distribution along the cut a–a' in Fig. 2(a).

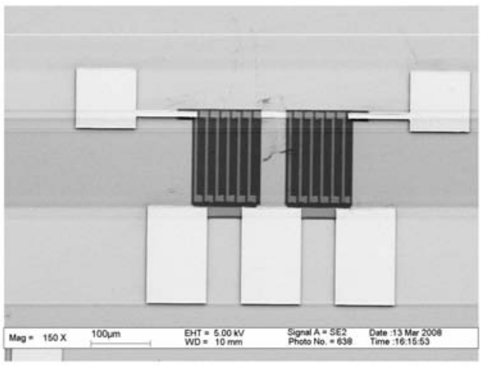

Fig. 6. SEM photo of the microwave power sensor.

3. Fabrication

The CPW was made of a 2 μm thick gold layer. The thermopiles consisted of gold and n^+ GaAs. The gold strips of the thermopiles were made by the sputtering of a 0.3 μm thick gold layer, and the n^+ GaAs was made from a 0.25 μm thick epitaxial layer. By using a lift-off process through depositing of a TaN layer, the matched loads were made with a square resistance of 25 Ω/□. The Seebeck coefficient of each thermocouple is 100 μV/K. A microphotograph of the microwave power sensor is shown in Fig. 6.

4. Experimental results

Measurements were performed at frequencies up to 20 GHz using an Agilent E8257D PSG Analog Signal Generator, an Agilent 8719ES Network Analyzer, a Cascade Microtech 1200 probe station for contacting the sensor, and an accurate DC voltage meter. Figure 7 shows the microwave performance of the sensor. Figure 7(a) shows an acceptable mismatch error below −26 dB in the experiment frequency range. The frequency response is shown in Fig. 7(b) at a constant power of 20 dBm. In the low frequency range, the output voltage oscillates considerably. Above 5 GHz, the response is more stable and the output voltage is lower than that in the low frequency range. The considerable losses in the high frequency range perhaps resulted from the fabrication process, since the GaAs substrate was not selectively etched very well. However, considering that the frequency at which the sensor would be used is larger than 5 GHz, the frequency response is acceptable.

The relationship between the output voltage and the

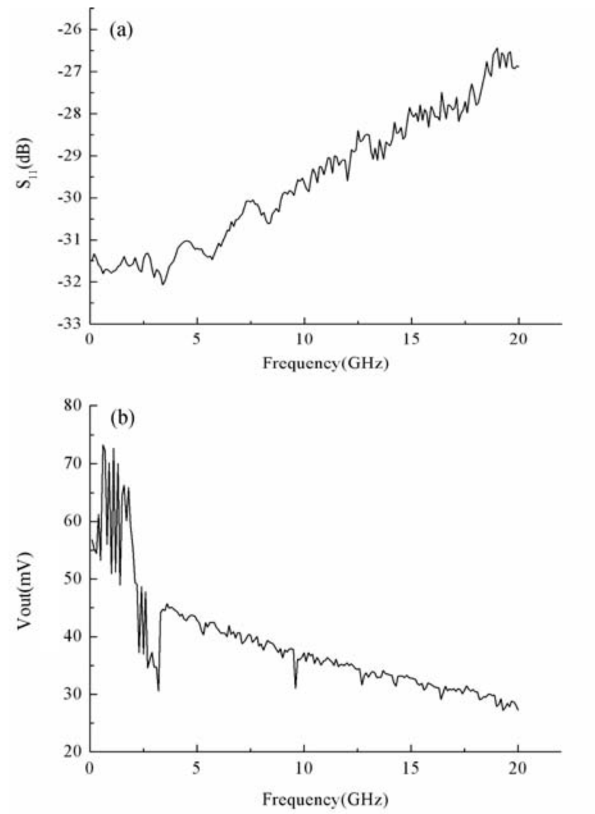

Fig. 7. Microwave performance: (a) Reflection loss of the microwave sensor; (b) Frequency response of the microwave sensor.

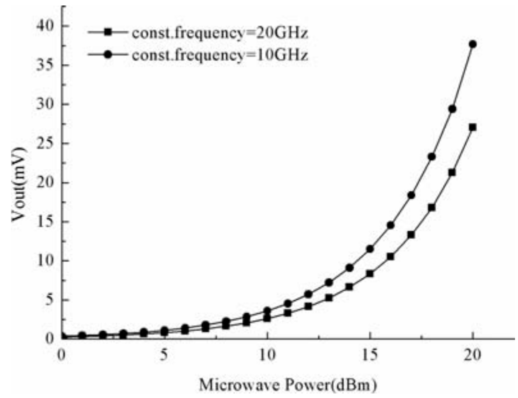

Fig. 8. Output voltage versus input power.

microwave power can be found in Fig. 8. Microwave intensities up to 20 dBm at 10 and 20 GHz were applied at the input, respectively, and the output DC voltages were recorded. The sensitivity is 0.37 mV/mW at 10 GHz and 0.27 mV/mW at 20 GHz. Because the thickness of the substrate used in the simulation is not exactly equal to the actual thickness, the differences between the results of the simulation and the experiment are understandable. However, the model is also useful for estimating the dimensions of the layout and the sensitivity.

In the heat transfer process, the CPW acts as a large heat sink, and some heat flow generated by the loads transfers to the CPW, resulting in a decrease of the temperature of the termination loads. Therefore, four types of CPW were designed in order to improve the heat transfer efficiency and the sensitivity. The photos of the different types of CPW are given in Fig. 9. The measurement results are shown in Fig. 10. The sensitivity

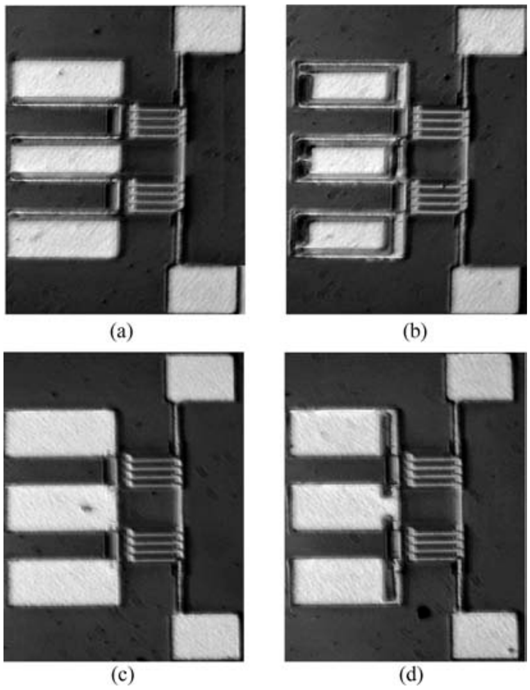

Fig. 9. Different types of CPW: (a) Type A; (b) Type B; (c) Type C; (d) Type D.

of type B at 20 dBm is nearly twice as large as the sensitivity of type D. The difference among types A, B, C and D is that there are some different thermally-isolated structures in A, B, and D. The difference in the structures is mainly due to the removal of some metal on the CPW. These structures will not destroy the electrical connection. With these thermally-isolated structures, less heat is transferred to the CPW, while the temperature difference between the hot junctions and cold junctions will be increased. As a result, the sensitivity will be improved. In other words, the microwave match performance of the CPW in types A, B and D is changed. Figure 10 is the result of the comprehensive action of heat transfer and microwave performance. Trade-off needs to be considered in the design process. The results were measured at a constant frequency of 10 GHz. There are eight thermocouples present in the sensor shown in Fig. 9, and twelve thermocouples in the sensor of Fig. 6. So the result in Fig. 8 is better than that in Fig. 10.

5. Conclusion

A terminating type MEMS microwave power sensor based on MMIC was proposed. An electrothermal model was

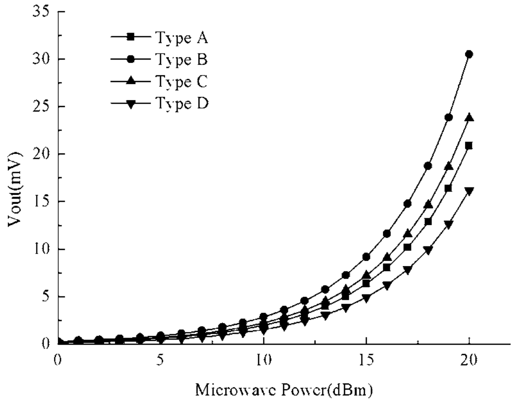

Fig. 10. Sensitivity of the microwave sensors with different CPW types.

introduced to simulate the heat transfer and temperature distribution, and the simulation results for the sensitivity were given. The measurement results showed that the reflection loss is less than –26 dB over the entire frequency range, and the sensitivity is 0.27 mV/mW at 20 GHz. In order to improve the sensitivity, four different types of CPW were designed. As a result, the sensitivity is nearly increased by a factor of 2.

References

[1] Milanovic V, Gaitan M, Bowen E D, et al. Thermoelectric power sensor for microwave applications by commercial CMOS fabrication. IEEE Electron Device Lett, 1997, 18(9): 450

[2] Milanovic V, Gaitan M, Bowen E D, et al. Implementation of thermoelectric microwave power sensors in CMOS technology. IEEE International Symposium on Circuits and Systems, 1997, 4: 2753

[3] Milanovic V, Gaitan M, Zaghloul M E. Micromachined thermocouple microwave detector in CMOS technology. IEEE 39th Midwest Symposium on Circuits and Systems, 1996, 1: 273

[4] Swart N R, Nathan A. Flow-rate microsensor modeling and optimization using SPICE. Sensors and Actuators A, 1992, 34: 109

[5] Milanovic V, Hopcroft M, Zincke C A, et al. Optimization of CMOS MEMS microwave power sensors. ISCAS, 1999, 5: 144

[6] Kozlov A G. Optimization of thin-film thermoelectric radiation sensor with comb thermoelectric transducer. Sensors and Actuators A, 1999, 75: 139

[7] Kozlov A G. Optimization of thin-film thermoelectric radiation sensor with separate disposition of absorbing layer and comb thermoelectric transducer. Sensors and Actuators A, 2000, 84: 259